Volume 4, Issue 2(2016) 557-570 ISSN 2347 - 3258
International Journal of Advance Research and Innovation

Application of Box Behnken design in Machining of turning samples of MMC

V.Shukla, A. Maheshwari
Department of Mechanical Engineering, IILM Academy of Higher Learning, Greater Noida Greater, Noida (UP) India

Article Info
Article history:
Received 25 January 2016
Received in revised form
20 February 2016
Accepted 28 February 2016
Available online 15 June 2016

Keywords:
Metal–matrix, Reynolds, Sommer feld number, Couple stress fluid

Abstract
Fabrication of AA6351/Al_2O_3 metal matrix composites with different percentage of reinforcement by stirs carting method. Microstructure observations of all fabricated samples were done to observe distribution of reinforcement. Investigations of mechanical properties of all sample effect of turning parameters on dimensional deviation of metal matrix composites.

1. Introduction

Matrix material strongly influences composite's overall transverse modulus, shear properties, and compression properties. Matrix material also significantly limits a composite's maximum permissible operating temperature. Most of the matrix materials are relatively lighter, more compliant, and weaker vis-à-vis fibers and whiskers. However, the combination of fibers/whiskers and matrix can be very stiff, very strong, and yet very light. Thus most of modern composites have very high specific strengths, i.e. very high strength/density ratios. This makes them very useful in aerospace applications, where weight minimization is a key design consideration. Fibers and whiskers in composites are held together by a binder known as matrix. This is required since fibers by themselves given their small cross-sectional area, cannot be directly loaded. Further they cannot transmit load between themselves. This limitation is addressed by embedding fibers in a matrix material. Matrix material serves several functions, the important ones being binds fibers together. Transfers loads and stresses within the composite structure and support the overall structure and protects the composite from incursion of external agents such as humidity, chemicals, etc. and protects fibers from damage due to handling.

Thiagarajan Rajmohan et al [1] studied the application of response surface methodology (RSM) and central composite design (CCD) for modeling, optimization, and an analysis of the influences of dominant machining parameters on thrust force, surface roughness and burr height in the drilling of hybrid metal matrix composites produced through stir casting route.S. Naher et al [2] showed many factors which influence the incorporation of particulate in metal matrix composites (MMCs). This paper presents work which examines the effect of viscosity during Al–SiC MMC production. Processing periods (up to 65 min), stirring speeds (50–500 rpm), and re-inforcement sizes (13–100 lm) for two different viscosity levels (1 and 300 mPa s) were investigated. S. Tzamtzis et al [3] observed that Particulate metal matrix composites (PMMCs) have attracted interest for application in numerous fields.S.K. Chaudhury et al [4] studied the frictional and wear behavior of Al–2Mg–11TiO2 composites prepared through spray forming and stir casting techniques are studied.Comparing with the Newtonian case, the couple stress effects of fluids containing suspensions provide an enhancement in the load capacity, as well as a reduction in the attitude angle and the friction parameter. D. Mandal et al [5] investigated the wear properties on 2.5, 5 and 10 wt% copper-coated short steel fiber reinforced Al–2Mg alloy composites fabricated by stir casting process were carried out using pin-on-disc wear testing apparatus. M. Baki Karamıs et al [6] studied extrusion die wear during the metal matrix composite (MMC) extrusion process was investigated with regard to the size of the reinforcement particle. T.V.S. Reddy et al [7] observed that this paper describes an attempt to enhance the wear properties of hypereutectic cast aluminium–silicon alloys produced by semi-solid metal (SSM) processing technique. Luca Casamichele et al [8] observed that indentation tests were performed on a large automotive component (a van gearbox) by means of a FIMEC apparatus. M.Emamy et al [9]developeda new technique in an aluminum based metal matrix composite in order to reveal the mechanism of formation of TiB_2 particles by mixing molten master alloys i.e., Al–8Ti and Al–4B in the Ti:B weight ratio of 5:2. A composite containing fine TiB2 particles produced by this technique.X.J. Wang et al [10] observed that the fracture behavior of SiCp/AZ91 magnesium matrix composite fabricated by stir casting is investigated using the in situ SEM technique.T.P.D. Rajan et al [11] observed that the effect of three different stir casting routes on the structure and properties of fine fly ash particles (13 lm average particle size) reinforced Al–7Si–0.35Mg alloy composite is evaluated. Among liquid metal stir casting, compocasting (semi solid processing), modified compocasting and modified compocasting followed by squeeze casting routes evaluated, the latter has resulted in a well-dispersed and relatively agglomerate and porosity free fly ash particle dispersed composites.L.Ceschini et al [12] observed that The use of aluminium-based particulate reinforced MMCs for automotive components and aircraft structures have been shown to be highly advantageous over their unreinforced alloys, due to their high specific strength and stiffness and superior wear resistance in a wide temperature range.S. Naher et al [13] proposed that Non-homogeneous particle

Corresponding Author,
E-mail address: vib.gla@gmail.com; abhishek.kumar@iilm.ac.in

distribution is one of the greatest problems in casting metal matrix composites (MMCs).S.M. Olhero et al [14] observed that in the present work rheological properties of aqueous concentrated AlN suspensions have been investigated in the presence of a sintering aid, deffloculant, binder and plasticizers, in order to screen the most suitable experimental conditions to obtain a good rheological behavior for tape casting thick and non-cracked tapes with good flexibility. Suspensions exhibiting the desired shear thinning behavior could be prepared. S. Balasivanandha Prabu et al [15] observed that high silicon content aluminium alloy–silicon carbide metal matrix composite material, with 10%SiC were successfully synthesized, using different stirring speeds and stirring times.YucelBirol et al [16] studied cooling slope (CS) casting process was employed in the present work to produce A357 thixo forming feedstock. K. Mahadevan et. al [17] observed that aluminium matrix-based discontinuously reinforced composites are age hardenable and can be strengthened through precipitation hardening process.Mohamed A.Taha et al [18] observed that Theworkability of aluminium–SiC and Al2O3-reinforced metal matrix composites (APMMCs) prepared by stir-casting, squeeze-casting and powder metallurgy techniques have been studied by using up-set test. T.Sornakumar et al [19] proposed that Bronze–alumina metal matrix composites have been attracting the interest of researchers in recent years, as they have many advantageous characteristics.Arda Cetin et al [20] observed that the damage and deformation behaviour of particulate reinforced metal matrix composites (PMMCs) can be highly sensitive to local variations in spatial distribution of reinforcement particles, which markedly depend on melt processing and solidification stages during production of PMMCs.

From the literature review it was observed that very few researchers investigate the effect of CNC turning parameters on dimensional deviation of AA6351/Al_2O_3 metal matrix composites. Objective of the present work was the fabrication of AA6351/Al_2O_3 metal matrix composites with different percentage of reinforcement by stir carting method. Microstructure observation of all fabricated samples was done to observe distribution of reinforcement. Investigations of mechanical properties of all samples and effects of turning parameters on dimensional deviation of metal matrix composites were analyzed.

2. Materials and Methods

2.1 Matrix Material

Most of the aerospace structures and its allied infrastructure are made of aluminum alloy. In this context considering Al 6351 which was used for making pressure vessel cylinders is now testing for aircraft structures. Al 6351 has high corrosion resistance and can be seen in forms of extruded rod bar and wire and extruded shapes. It is easily machinable and can have a wide variety of surface finishes. It also has good electrical and thermal conductivities and is highly reflective to heat and light. Due to the superior corrosion resistance, Al 6351 offers extremely low maintenance. Al 6351 is only one-third the weight of cast iron, with about 75% of comparable tensile strength. Early research was done on crack phenomenon of hallow cross sectional specimen only. In this investigation the tensile strength on circular rod specimen of Al 6351 is finding out by applying the loads on universal testing machine with various dimensions. The experimental results were found satisfactory to propose the alternative alloy for aircraft structures. The mechanical and physical properties of aluminum alloy (6351) have been reviewed from literature data for the purpose of characterizing the mechanical for manufacturing process in engineering application. Aluminum alloys are used in many applications in which the combination of high strength and low weight is attractive in air frame in which the low weight can be significant value. Al 6351 is known for its light weight (density = 2.7g/cm3) and good corrosion resistance to air, water, oils and many chemicals. Thermal and electrical conductivity is four times greater than steels. The chemical compositions of Al 6351 are Si-0.93,Fe-0.36, Cu-0.1, Mn-0.57, Mg-0.55, Zn 0.134, Ti- 0.014 and remaining Al. It has higher strength amongst the 6000 series alloys. Alloy 6351 is known as a structural alloy, in plate form. This alloy is most commonly used for machining. Though relatively a new alloy the higher strength of 6351 has replaced 6061 alloy in many applications. Mechanical properties can be easily obtained at tension tests, with great accuracy. Thus, alloy such as 6351 have significantly more silicon than magnesium or other elements, but find themselves in the Mg_2Si series. The AA 6351 aluminum alloy is used in manufacturing due to its strength, bearing capacity, ease of workability and weldability. It is also used in building boat, column, chimney, rod, mould, pipe, tube, vehicle, bridge, crane and roof. One of the most important properties of AA 6351 aluminum alloy is that the treatment of solid solution is not so critical. One of the major areas of Al 6351 for investigating crack phenomena is the gas cylinders made of this material often prone to crack at various tensile residual stresses. Sustained load cracking, a metallurgical anomaly, occasionally develops in 6351 aluminum alloy high-pressure cylinders. The advantages of Al 6351 have several important performance characteristics that make them very attractive for aircraft structures, namely light unit weight, only one third that of steel, strength comparable to typical other aluminum alloys, excellent corrosion resistance, with negligible corrosion even in the presence of rain and other drastic

Table 1: Properties of aluminum alloy (6351)

aluminum alloy	copper	magnesium	Silicon	iron	Manganese	Others
6351	0.1%	0.4-1.2%	0.6-1.3%	0.6%	0.4-1.0%	0.3%
aluminum alloy	copper	magnesium	Silicon	iron	Manganese	Others
6351	0.1%	0.4-1.2%	0.6-1.3%	0.6%	0.4-1.0%	0.3%

conditions, high toughness and resistance to low-ductility fracture even at very low temperatures and free of any ductile-to-brittle transition that has sometimes been fatal to older structures and excellent fabric ability. These performance characteristics provide significant advantages over conventional aircraft design, fabrication and erection of aerospace structures like light weight and comparable strength enables the use of a higher ratio of live load to dead load, superior corrosion resistance resulting in lower maintenance costs, superior low-temperature toughness eliminates concerns about brittle fracture even in the most severe arctic weather, ease of extrusion enables the design of more weight-efficient beam and component cross sections, placing the metal where it is most needed within a structural shape or assembly including providing for interior stiffeners and for joints and the combination of light weight and ease of fabrication.

2.2 Reinforcement Material

Aluminum oxide (Al_2O_3) is widely used as the reinforcing additive in the metal matrix composites. The influence of Al2O3 particle size on the density, hardness, microstructure, yield stress, compression strength, and elongation of the sintered Al–Al_2O_3 composites were investigated. The grain size and particle distribution homogeneity was decreased with raising the particle size.The mechanical and physical properties of alumina (Al_2O_3) have been reviewed from literature data for the purpose of characterizing the mechanical properties of alumina for manufacturing process in engineering application.

Metal–matrix composites (MMCs) are most promising in achieving enhanced mechanical properties such as: hardness, Young's modulus, 0.2% yield strength and ultimate tensile strength due to the presence of micro-sized reinforcement particles into the matrix. Generally, regards to the mechanical properties, the reinforcements result in higher strength and hardness, often at the expense of some ductility. Aluminum-matrix composites (AMCs) reinforced with particles and whiskers are widely used for high performance applications such as in automotive, military, aerospace and electricity industries because of their improved physical and mechanical properties. In the composites relatively soft alloy like aluminum can be made highly resistant by introducing predominantly hard but brittle particles such as Al_2O_3 and SiC.

Table 2: Mechanical properties of (Al_2O_3)

Material	Sample 1	Sample 2	Sample 3	Sample 4
aluminium alloy (AA6351)	97.5%	95%	92.5%	90%
aluminium oxide (Al_2O_3)	2.5%	5.0%	7.5%	10%

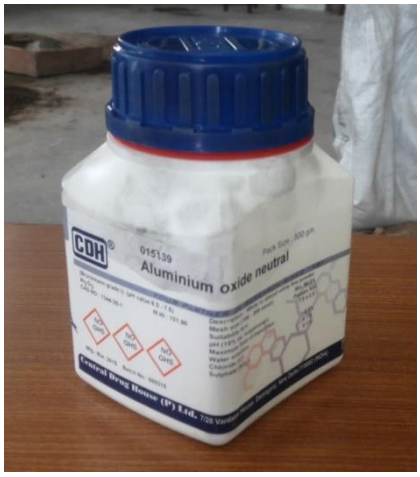

Fig.1: Reinforcement (Al_2O_3)

Among Al-alloys, 6351Al-alloy is widely used in numerous engineering applications including transport and construction where superior mechanical properties such as tensile, strength, hardness etc., are essentially required. Hard particles such as B_4C, Al_2O_3 and SiC are commonly used as reinforcement phases in the composites. The application of Al2O3 particle reinforced aluminum alloy matrix composites in the automotive and aircraft industries is gradually increasing for pistons, cylinder heads, connecting rods etc. where the tribological properties of the materials are very important. In addition, the mechanical properties of MMCs are sensitive to the processing technique used to fabricate the materials. Considerable improvements may be achieved by applying science-based modelling techniques to optimize the processing procedure. Several techniques have been employed to prepare the composites including powder metallurgy, melt techniques and squeeze casting.

2.3 Experimental Procedure

The work materials used in the present work are aluminium alloy (AA6351) and aluminium oxide (Al_2O_3 as reinforcement). These materials are chosen due to their easily mixable property and gives good mechanical properties. First of all the aluminium alloy (AA6351) is heated upto its melting temperature in a electric furnance and then aluminium oxide is heated and mixed slowly in molten aluminium alloy with the help of stirrer. The mixer is left for cool down in the crucible in which it was melted and mixed. There are four samples in different ratios which are prepared for testing mechanical properties and choosing the best. The ratios are shown below in the Table 3.

Table 3: Composition selection

Alumina (Al_2O_3)	Grade	pH value	Mesh size	Min.
Neutral(1344-28-1)	Brockman 1 or 2	6.5-7.5	100-300	90%

Fig.2: Electric furnance

Fig.3: Mechanical stirrer

Now the mixed composite after cooling is cutted into desired shapes for testing mechanical properties on the cutting machine. The cutting machine is an electrically driven machine which is used to cut the hard composites. The MMC samples prepared are shown in figures given below.

Fig.4: MMC (2.5% of Al_2O_3)

The Machine on which these prepared samples are cutted is shown in the figure given below: The MMC samples prepared for mechanical properties testing after cutting and finshing are shown in the figures: After preparing all the MMC sample mechanical properties like testing of hardness, toughness and tensile strength are to be performed on their respective testing machines for determining the best one in properties among all of the different ratio samples and selecting the strongest one.

Fig. 5: MMC (5% of Al_2O_3)

Fig.6: MMC (7.5% of Al_2O_3)

Fig.7: MMC (10% of Al_2O_3)

2.4 Response Surface Methodology

Response surface methodology (RSM) is a collection of mathematical and statistical techniques for empirical model building. By careful design of experiments, the objective is to optimize a response (output variable) which is influenced by several independent variables(input variables). An experiment is a series of tests, called runs, in which changes are made in the input variables in order to identify the reasons for changes in the output response. Originally, RSM was developed to model experimental responses (Box and Draper, 1987), and then migrated into the modelling of numerical experiments. The difference is in the type of error generated by the response. In physical experiments, inaccuracy can be due, for example, to measurement errors while, in computer experiments, numerical noise is a result of incomplete convergence of iterative processes, round-off errors or the discrete representation of continuous physical phenomena (Giunta et al., 1996; van Campen et al., 1990,Toropov et al.,

Fig.8: Cutting machine

Fig.9: MMC sample prepared for hardness test

Fig.10: MMC sample for tensile test

Fig.11: MMC sample prepared for toughness test

Fig.12: MMC sample prepared for microstructure

1996). In RSM, the errors are assumed to be random.The application of RSM to design optimization is aimed at reducing the cost of expensive analysis methods (e.g. finite element method or CFD analysis) and their associated numerical noise. The problem can be approximated as described in with smooth functions that improve the convergence of the optimization process because they reduce the effects of noise and they allow for the use of derivative-based algorithms. Venter et al. (1996) have discussed the advantages of using RSM for design optimization applications.

For example, in the case of the optimization of the calcination of Roman cement engineer wants to find the

levels of temperature ($x1$) and time ($x2$) that maximize the early age strength (y) of the cement. The early age strength is a function of the levels of temperature and time, as follows:

$$y = f(x1, x2) + \varepsilon \quad (1)$$

where, ε represents the noise or error observed in the response y. The surface represented by $f(x1, x2)$ is called a response surface. The response can be represented graphically, either in the three-dimensional space or as contour plotsthat help visualize the shape of the response surface. An important aspect of RSM is the design of experiments(Box and Draper, 1987), usually abbreviated as DOE. These strategies were originally developed for the model fitting of physical experiments, but can also be applied to numerical experiments. The objective of DOE is the selection of the points where the response should be evaluated. Most of the criteria for optimal design of experiments are associated with the mathematical model of the process. Generally, these mathematical models are polynomials with an unknown structure, so the corresponding experiments are designed only for every particular problem. The choice of the design of experiments can have a large influence on the accuracy of the approximation and the cost of constructing the response surface.

3. Results and Discussion

3.1 Analyses of Microstructure

The microstructures of the MMC samples are seen using metallurgical microscope. When describing the structure of a material, we make a clear distinction between its crystal structure and its microstructure. The term 'crystal structure' is used to describe the average positions of atoms within the unit cell, and is completely specified by the lattice type and the fractional coordinates of the atoms. The term 'microstructure' in metal matrix composites is used to describe the appearance of the reinforcement material. A reasonable working definition of microstructure is the arrangement of phases and defects within a material. Uniform distribution was observed of all selected composition.

3.2 Analyses of Tensile Strength

The tensile testing of MMC Composite is carried out on tensometer machine. Tensometer is a device used to evaluate the tensile properties of materials such as their Young's modulus and tensile strength. It is usually a universal testing machine loaded with a sample between two grips that are either adjusted manually or automatically to apply force to the specimen. The machine works either by driving a screw or by hydraulic ram. Testing is done by clamping the specimen in the jaws of the tensometer. The load is applied gradually and the material starts elongating. After the maximum load reached the specimen breaks. The data collected from the tensile test by tensometer has been graphically shown:-

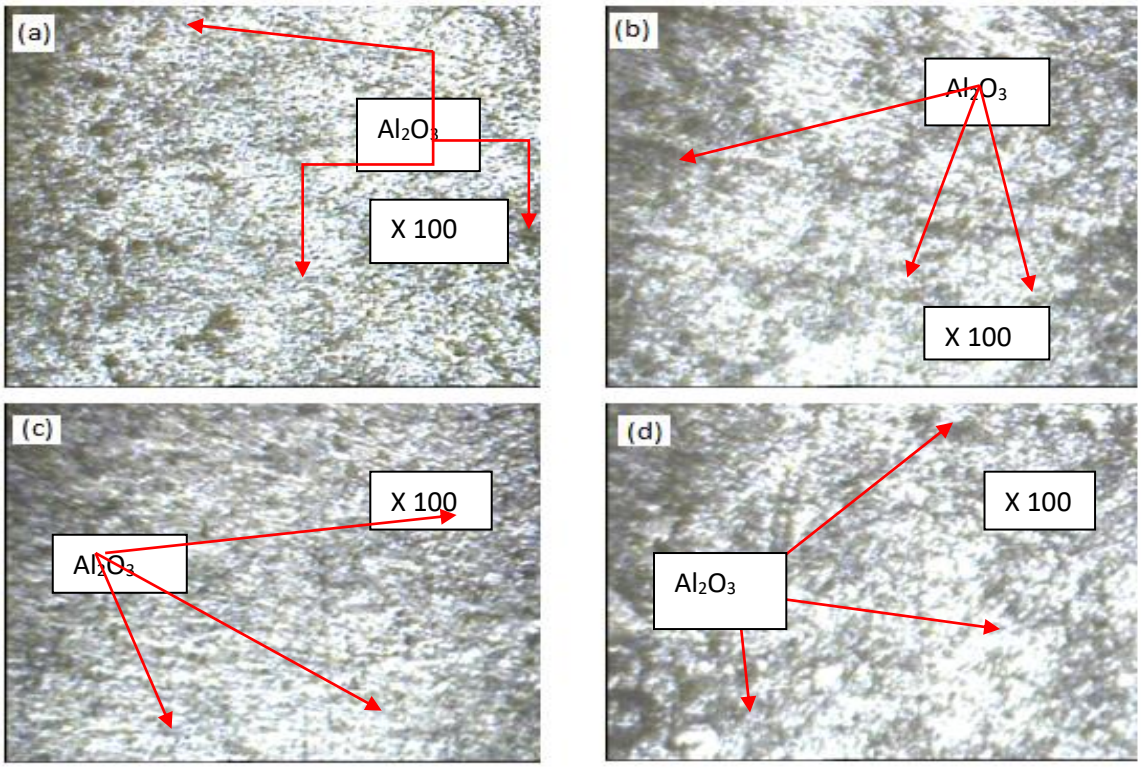

Fig 5: (a) 2.5 % reinforcement, (b) 5 % reinforcement, (c) 7.5 % reinforcement, (d) 10 % reinforcement

Fig 5 Sample of MMC (a) Before Testing (b) After Testing

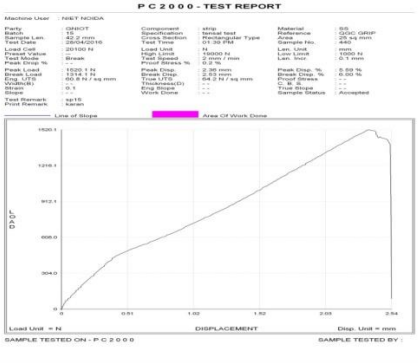

Fig.8: Tensile Test of 7.5% of Al2O3 mixed with Al

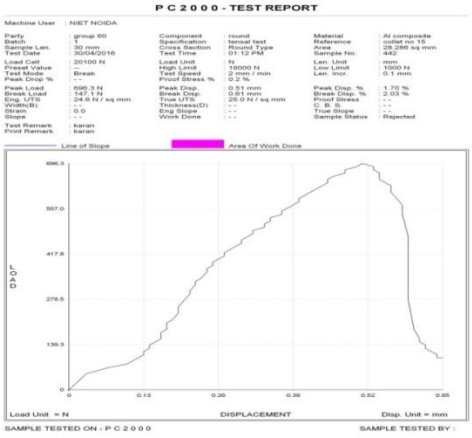

Fig.6: Tensile test of 2.5% of Al_2O_3 mixed with Al

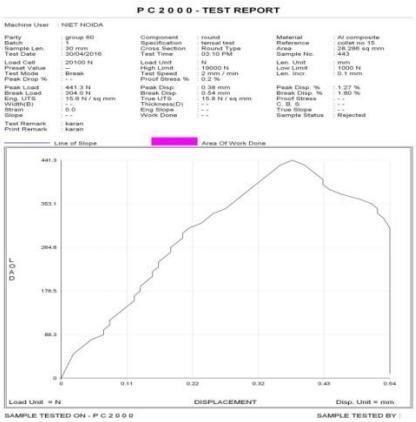

Fig. 9: Tensile Test of 10% of Al2O3 mixed with Al

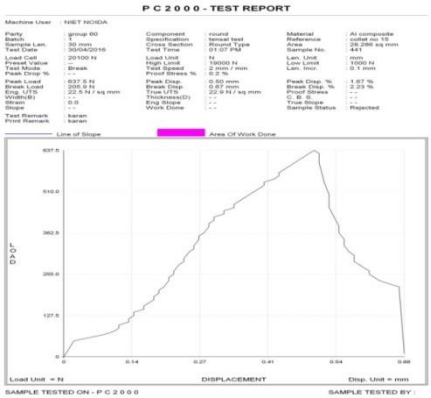

Fig.7: Tensile Test of 5% of Al_2O_3 mixed with Al

Fig10: MMC sample after toughness testing

Table 4: Tensile of MMC

Samples (of Al_2O_3)	Ultimate strength (N)	Elongation (mm)	Break load (N)	Break Elongation (mm)	True UTS (N/ sq mm)	Area (sq. mm)
2.5%	696.3	0.51	147.1	0.61	25	28.286
5.0%	637.5	0.5	205.9	0.67	22.9	28.286
7.5%	1520.1	2.36	1314	2.53	64.2	25
10%	441.3	0.38	304	0.54	15.8	28.286

3.3 Analysis of Toughness Test

In these MMC specimens toughness is tested by breaking it with impacting force of a hammer weighing 21 kg. The Hammer is leaved from 140 degree of angle with the initial energy of 300 J. The table shows the results while testing as shown in figure.

Table 4: Toughness of MMC

Composition	2.5% of Al_2O_3(Energy in J)	5% of Al_2O_3(Energy in J)	7.5% of Al_2O_3 (Energy in J)	10% of Al_2O_3(Energy in J)
Sample 1	6	4	8	14
Sample 2	6	4	6	10

3.4 Analysis of Hardness Test

The hardness test was carried on Rockwell Hardness testing method in which the hardness is determined by measuring the depth of an indentor under a large load compared to the penetration by the preload. Rockwell hardness values are expressed as a combination of a hardness number and a scale symbol representing the indenter and the minor and major loads. The hardness number is expressed by the symbol HR and the scale designation.

The of Principle of Rockwell test is indenter moves down into position on the part surface.A minor load is applied and a zero reference position is established. The major load is applied for a specified time period (dwell time) beyond zero. The major load is released leaving the minor load applied. It is calculated as:

$$BHN = \frac{F}{\frac{\pi}{2} D * \left(D - \sqrt{D^2 - Di^2}\right)}$$

Where: F is force used in KgF

D is the diameter of the indenter in mm

Di is the diameter of the indentation in mm

Table 5 Hardness of MMC

Compositions	2.5% of Al_2O_3 (Hardness in BHN)	5% of Al_2O_3 (Hardness in BHN)	7.5% of Al_2O_3 (Hardness in BHN)	10% of Al_2O_3 (Hardness in BHN)
Sample 1	49	44	49	40
Sample 2	42	32	44	49

Fig. 12 MMC sample after indentation on hardness testing machine

4. Dimensional Deviation

As manufacturing companies pursue higher-quality products, they spend much of their efforts monitoring and controlling dimensional accuracy dimensional deviation prediction of workpiece in turning of MMC samples like spindle speed, feed rate, depth of cut, pressure of cooling lubrication fluid and number of produced parts were taken as input parameters and dimensional deviation of workpiece as an output parameter. Importance of a single parameter and their interactive influences on dimensional deviation were statistically analyzed and values predicted from regression. The principal goal of this paper was to investigate the influence of depth of cut, cutting speed and feed rate on the dimensional (length, diameter and radius) and geometric (parallelism and angularity) deviations obtained after turning of MMC samples. The quality of moulds and dies subjected to milling is significant to the final cost of these products due to the influence of milling on subsequent finishing and polishing operations. Therefore, better quality rough and semi-finish mills operations result in shorter finishing and polishing cycles and lower manufacturing costs. The principal strategies used to optimize both productivity and surface quality when milling hardened die and mould materials at high speeds. Contour milling is the most common approach employed when roughing to achieve higher metal removal rates associated with less machining time. While finishing milling, number of factors must be taken into account, such as mould or die features, cutter geometry, the radial depth of cut and the cutter path strategy.

In addition, the use of adaptive machining to maintain a consistent cutting load by changing cutting speed, depth of cut and feed rates may result in an improved surface finish and higher productivity. But milling forces change considerably during one rotation of a cutter due to variations in chip thickness. The stability of metal cutting operations at low spindle speeds are challenging to model mainly because of the difficulty in predicting the process damping. Consequently, the clearance face of the tool rubs against the waves causing frictional forces against the direction of motion which damp out chatter vibrations additionally to the machining parameters, tool geometry and work material properties, the following parameters must be considered in order to accurately predict milling forces: cutting temperature variation, cutter run out, cutter and workpiece vibrations. When cavities are machined, tool deflection changes with the cutter path, especially in

corners. To minimize this effect, lower width of cut values should be employed, thus diminishing the milling force components and consequently, tool deflection. For cutting corners the pocket milling is implemented as a module of a commercial CAD/CAM system. The high rotational speeds the centrifugal force presses the fingers against the inner wall of the cutter, resulting in a frictional force that reduces chatter vibrations. Tool deflection is considered to be the most critical factor that influences both surface finish and dimensional deviations, and for this reason, a number of researchers have ad-dressed this subject matter.

4.1 Experimental Design

The input process parameters for CNC turning that determine the properties of MMC are speed of cut, feed rate and depth of cut. The experiment is planned on the basis of three- factor five-level central composite rotatable design, with full imitation. Design-Expert Box Benhken is used to conduct statistical analysis, to develop mathematical models and to optimize the process parameters. The selected process parameters and their limits, units and notations are given in Table 3.5. In the experiment, the Dimensional deviation is considered to evaluate the MMC composites.

Table 6 Process parameters

Parameters	Unit	Range
Speed	m/min	90-170
Feed rate	mm/rev	0.15-0.25
Depth of cut	Mm	0.18-0.54

Table 7 Design matrix

Std. order	Run order	Speed of cut	Feed rate	Depth of cut	Dimensional deviation
9	1	130	0.15	0.18	1.01
17	2	130	0.2	0.36	1.05
12	3	130	0.25	0.54	1.95
10	4	130	0.25	0.18	1.30
14	5	130	0.20	0.36	1.08
5	6	90	0.20	0.18	1.03
11	7	130	0.15	0.54	1.10
15	8	130	0.20	0.36	0.90
4	9	170	0.25	0.36	2.10
13	10	130	0.20	0.36	1.05
3	11	90	0.25	0.36	1.30
7	12	90	0.20	0.54	1.20
1	13	90	0.15	0.36	0.90
8	14	170	0.20	0.54	1.60
16	15	130	0.20	0.36	1.10
2	16	170	0.15	0.36	1.06
6	17	170	0.20	0.18	1.20

4.2 Development of Mathematical Model

The aim of Analysis of variance (ANOVA) is investigating whether the process parameters have significant effects on MMC composite properties and conducting quantitative analysis of the impact of various factors on experimental results, so as to specify whether the model developed is meaningful. The significance test of regression model and single model coefficients and distortion test are carried out by software Design-Expert V7. In order to make simpler, the quadratic model stepwise deterioration method is used to automatically delete the insignificant model conditions. MMC composite properties of the ANOVA analysis are shown in Table 6.

The ANOVA table indicates that the model terms can be considered as statistically significant. The ANOVA result shows that the speed of cut, feed rate and depth of cut are the significant model terms associated with Dimensional deviation. The other model terms are not important and thus eliminated by backward elimination process to improve model capability. It is apparent from the figure that strength increases with the CNC turning power, while the strength decreases at the excessive power. Increasing the CNC turning power increases the heat input to the material, resulting in increased strength. It can also be observed from this plot that the turning speed has a negative effect on the strength. Because a higher turning speed lowers the irradiation time, causing low-heat input to the composites, as a result, the strength decreases. This plot also indicates that the radiation area increases with the increase of the stand-off-distance, resulting in the increase of the strength until it reaches its center value, the strength then starts to decrease with the increase of stand-off-distance beyond the center limit as a result of lower power density. Series of process parameters meeting the optimization standards are obtained in the mathematical model, which has been optimized by the Design-Expert V7. Three groups of optimized parameters are selected randomly to conduct confirmation experiments in order to validate the mathematical model. Repeat it three times for each group, the actual value of the results is calculated as the average of

three trials. Table 3.5 lists the actual values, mathematical model predictions and calculated percentage error of confirmation experiments.

Table 8 ANOVA Table

Source	Sum of squares	DF	Mean square	F value	Prob>F	
Model	1.82	9	0.20	22.43	0.0002	Significant
A	0.27	1	0.27	30.01	0.0009	
B	0.83	1	0.83	92.46	<0.0001	
C	0.23	1	0.23	26.07	0.0014	
A^2	0.059	1	0.059	16.14	0.0377	
B^2	0.15	1	0.15	6.54	0.0051	
C^2	0.059	1	0.059	11.38	0.0377	
AB	0.10	1	0.10	0.80	0.0119	
AC	7.225E-003	1	7.225E-003	8.71	0.4000	
BC	0.078	1	0.078		0.0214	
Residual	0.063	7	8.999E-003			
Lack of fit	0.038	3	0.013	2.04	0.2513	Not Significant
Pure error	0.025	4	6.230E-003			
Cor Total	1.88	16				

It can be observed from the validation experiments that there is a small percentage error between the estimated and the experimental values, which indicates that the developed models can yield nearly accurate results. The relationship between the predictable and the experimental values of the composites strength Figure 22. It is indicated from the figures that the developed models are adequate and predicted values are in good agreement with measured data. As the turning power increases, the composites strength and the deviation increase, whereas the accuracy decreases with increased turning speed. The accuracy increases with the increase of the stand-off- distance until it reaches the center value, the strength then starts to decrease with the increase of stand-off-distance beyond the center limit. On the other hand, accuracy gradually increases with the stand-off-distance in the whole design space. The confirmation experiment results indicate that the predicted values obtained by the mathematical model are in good agreement with the actual values.

It can be observed from the validation experiments that there is a small percentage error between the estimated and the experimental values, which indicates that the developed models can yield nearly accurate results. The relationship between the predictable and the experimental values of the composites strength Figure 22. It is indicated from the figures that the developed models are adequate and predicted values are in good agreement with measured data. As the turning power increases, the composites strength and the deviation increase, whereas the accuracy decreases with increased turning speed. The accuracy increases with the increase of the stand-off- distance until it reaches the center value, the strength then starts to decrease with the increase of stand-off-distance beyond the center limit. On the other hand, accuracy gradually increases with the stand-off-distance in the whole design space. The confirmation experiment results indicate that the predicted values obtained by the mathematical model are in good agreement with the actual values.

Table 9: Std. Deviation

Std. Deviation	0.095	R-Squared	0.9665
Mean	1.23	Adj R-Squared	0.9234
C.V.	7.68	Pred R-Squared	0.6552
PRESS	0.65	Adeq Precision	14.380

The Model F-value of 22.43 implies the model is significant. There is only a 0.02% chance that a "Model F-Value" this large could occur due to noise. Values of "Prob > F" less than 0.0500 indicate model terms are significant. In this case A, B, C, A^2, B^2, C^2, AB, BC are significant model terms. Values greater than 0.1000 indicate the model terms are not significant. If there are many insignificant model terms (not counting those required to support hierarchy), model reduction may improve your model. The "Lack of Fit F-value" of 2.04 implies the Lack of Fit is not significant relative to the pure error. There is a 25.13% chance that a "Lack of Fit F-value" this large could occur due to noise. Non-significant lack of fit is good -- we want the model to fit.

The "Pred R-Squared" of 0.6552 is not as close to the "Adj R-Squared"of 0.9234 as one might normally expect. This may indicate a large block effect or a possible problem with your model

and/or data. Things to consider are model reduction, response tranformation, outliers, etc. "Adeq Precision" measures the signal to noise ratio. A ratio greater than 4 is desirable. Ratio of 14.380 indicates an adequate signal. This model can be used to navigate the design space.
The "Pred R-Squared" of 0.6552 is not as close to the "Adj R-Squared" of 0.9234 as one might normally expect. This may indicate a large block effect or a possible problem with your model and/or data. Things to consider are model reduction, response tranformation, outliers, etc. "Adeq Precision" measures the signal to noise ratio. A ratio greater than 4 is desirable. Your ratio of 14.380 indicates an adequate signal. This model can be used to navigate the design space.

Table 10 Diagnostics Case Statistics

Std. Order	Actual Value	Predicted Value	Residual
1	0.90	0.99	-0.094
2	1.06	1.04	0.019
3	1.30	1.32	-0.019
4	2.10	2.01	0.094
5	1.03	0.96	0.070
6	1.20	1.24	-0.043
7	1.26	1.22	0.042
8	1.60	1.67	-0.070
9	1.01	0.99	0.024
10	1.30	1.35	-0.051
11	1.10	1.05	0.051
12	1.95	1.97	-0.024
13	1.05	1.04	0.014
14	1.08	1.04	0.044
15	0.90	1.04	-0.14
16	1.10	1.04	0.064
17	1.05	1.04	0.014

4.4.1Normal% Probability and Studentized Residual

A normal probability plot is found by plotting the residuals of the observed sample against the corresponding residuals of a standard normal distribution $N(0,1)$. If the plot shows a straight line, it is reasonable to assume that the observed sample comes from a normal distribution. If the points deviate a lot from a straight line, there is evidence against the assumption that the random errors are an independent sample from a normal distribution. Independence (response variables y_i are independent) this is a design issue and Normality (response variables are normally distributed). Look at the residuals plot. Notice that the residuals are not symmetrically distributed about zero. They are mostly positive with low and high values of predicted Y and mostly negative with medium values of predicted Y. If you were to find the means of the residuals at each level of Y and connect those means with the line you would get a curve with one bend. This strongly suggests that the relationship between X and Y is not linear and you should try a nonlinear model.

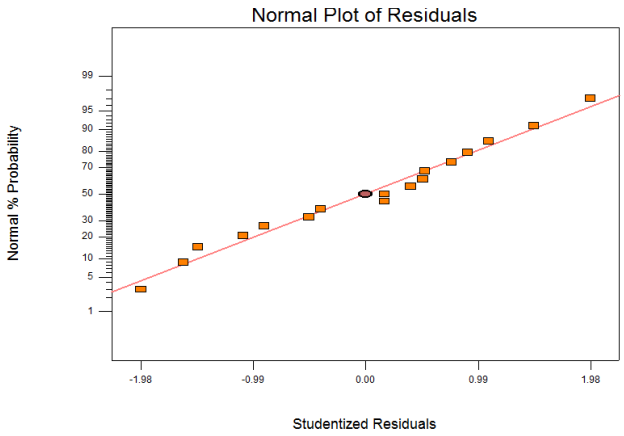

Fig.13: Graph normal% probability vsstudentizedresidual

Notice that the problem is not apparent when we look at the marginal distribution of the residuals. Following any modeling procedure, it is a good idea to assess the validity of your model. Residuals and diagnostic statistics allow you to identify patterns that are either poorly fit by the model, have a strong influence upon the estimated parameters, or which have a high leverage. The significant factors A, B, C, D, AB, AC, AD, BC, BD. Values of ‘‘p-value>F’’ less than 0.0500 shows model terms are statistically significant at 95% confidence level. Perturbation curve shows the effect of each process input parameter on mean cutting speed with a common point where all four input parameters meats to achieve max. mean cutting speed to interpret these diagnostics jointly to understand any potential problems with the model.

4.4.2 Predicted and Actual

Regression allows you to predict variables based on another variable. In this we will focus on linear regression or relationships that are linear (a line) rather than curvilinear (a curve) in nature. Let's begin with the example used in the text in which mental health symptoms are predicted from stress. Predicted Values select Unstandardizedand Standardized. For Residuals, also select Unstandardizedand Standardized. Now SPSS will save the predicted values of symptoms based on the regression equation and the residual or difference between the predicted values and actual values of symptoms in the data file.

4.5 Dimensional Deviation and Cutting Speed

Quadratic Vs two factors interaction (2FI) has been found the best fit model for cutting speed. From perturbation curve, it is clear that cutting speed increases with increase in value of Ton and current while Ton and current do not have major effect on dimensional deviation. Dimensional deviation decreases with increase in voltage and Toff. Using desirability function, parameters have been predicted for maximizing the machining speed and minimize dimensional deviation.

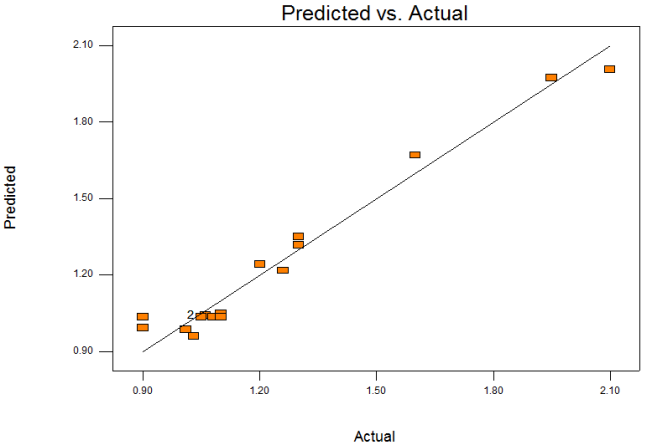

Fig. 14: Graph predicted vs actual

The goal of optimization is to find a good set of conditions that will meet the desired goal. It is not necessary that the value of desirability is always 1.0 as the value is completely dependent on how closely the lower and upper limits are set relative to the actual optimum value. The set of conditions possessing highest desirability value have been selected as optimum conditions for maximum cutting speed and minimum dimensional deviation. The constraints for the optimization of cutting speed have been shown in fig 3b by the help of ramp chart. Using Design expert (DX-9), optimal solutions have been derived for specified design space constraints for machining speed. Table 4 shows the set of conditions correspond to maximum desirability value for CS and minimum dimensional deviation.

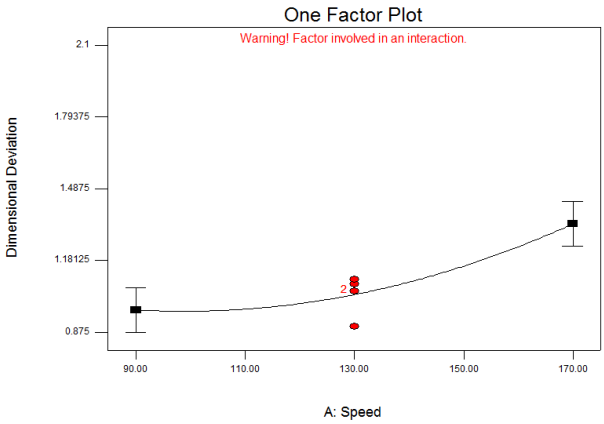

Fig.15: Graph dimensional deviation vs cutting speed

4.6: Dimensional Deviation and Feed Rate

Here in this, graph is plotted between dimensional deviation and feed rate which represents there characteristics towards each other. The graph signifies that where the feed rate is increased the dimensional deviation also increases due to which the accuracy is the reduced.

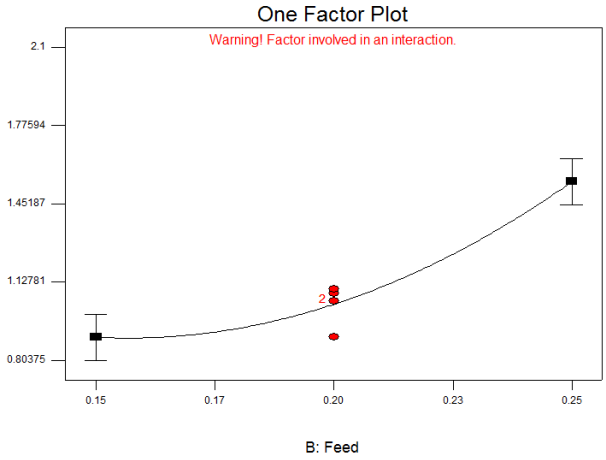

Fig.16: Graph dimensional deviation vs feed rate

4.7: Relationship between Dimensional Deviation and Depth of Cut

The experiments carried out during the reported work include cutting specimens by varying cutting parameters like Power and Depth of cut. The set of data obtained was useful in developing a model for predicting depth of cut for single pass cutting for various combinations of speed and power.

It was found that depth of cut increases with increase in power whereas depth of cut decreases with increase in speed. The variation of predicted model from the actual one may be due to the evaporation of material and getting settled back during the experiment. The variation in depth

data may be due to ineffective utilization of blower system. Since the specimens consist of blind holes, the removed material during machining may get settled down before evaporation by the blower and cause uncertainty in data.

4.8: 3 Dimensional Deviation Feed and Speed

Here in this, 3D graph the dimensional deviation, depth of cut and feed rate which represents there characteristics towards each other. The graph signifies that when the feed rate and depth of cut increases the dimensional deviation also increases due to which the accuracy is the reduced.

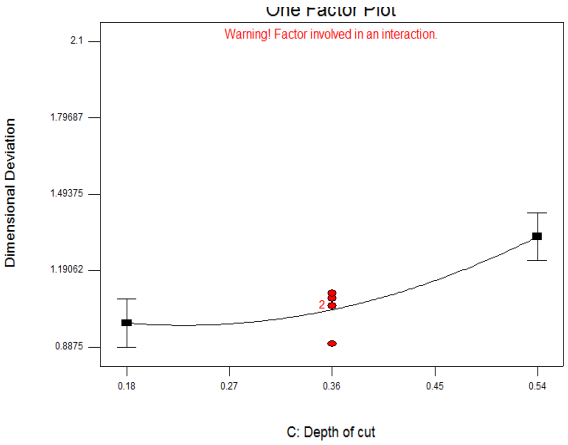

Fig.17: Graph dimensional deviation vs depth of cut

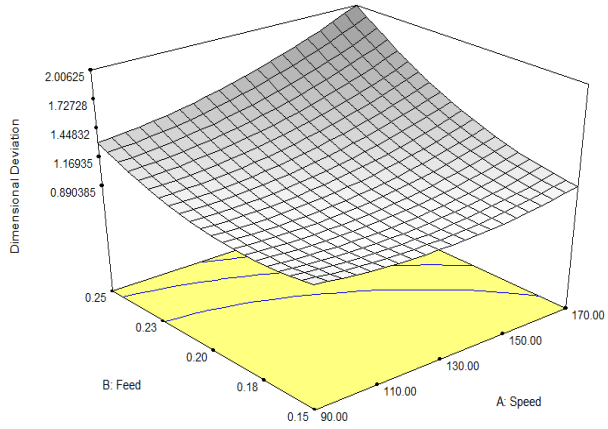

Fig.18: 3D Graph dimensional deviation, feed and speed

4.9 - 3 Dimensional Deviation, Doc and Speed

Here in this, 3D graph the dimensional deviation, depth of cut and speed which represents there characteristics towards each other. The graph signifies that when the speed and depth of cut increases the dimensional deviation also increases due to which the accuracy is the reduced.

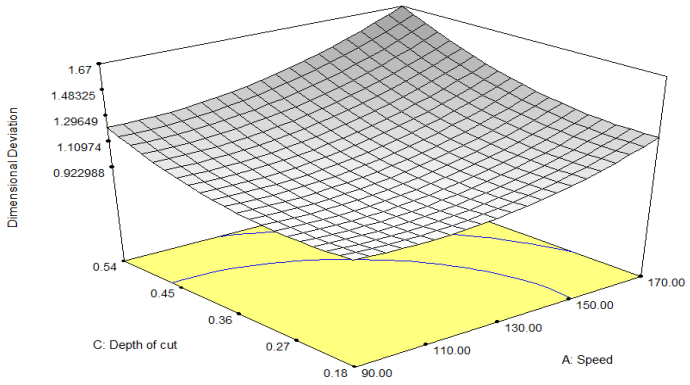

Fig.19: 3D deviation, doc and speed

Conclusions

In the present investigation, it was observed that maximum mechanical properties were obtained for AA6351/7.5% Al 2 O 3. The optimum process parameters were found to be cutting speed 90.00, feed rate of 0.15 and depth of cut of 0.18 to achieve minimum dimensional deviation 1.12323 with the desirability equals to 0.950. In the present investigation, it was observed that maximum mechanical properties were obtained for AA6351/7.5% Al 2 O 3. The optimum process parameters were found to be cutting speed 90.00, feed rate of 0.15 and depth of cut of 0.18 to achieve minimum dimensional deviation 1.12323 with the desirability equals to 0.950.

References

[1.] Thiagarajan Rajmohan, Kayaroganam Palanikumar, "Application of the central composite design in optimization of machining parameters in drilling hybrid metal matrix composites" ,Measurement 46, 2013, 1470–1481.

[2.] S. Naher , D. Brabazon , L. Looney, "Computational and experimental analysis of particulate distribution during Al–SiC MMC fabrication", Composites: Part A 38, 2007, 719–729.

[3.] S.Tzamtzis , N.S. Barekar , N. HariBabu , J. Patel , B.K. Dhindaw , Z. Fan, "Processing of advanced Al/SiC particulate metal matrix composites under intensive shearing – A novel Rheo-process", Composites: Part A 40, 2009, 144–151.

[4.] S.K. Chaudhury, A.K. Singh, C.S. Sivaramakrishnan, S.C. Panigrahi, "Wear and friction behavior of spray formed and stir cast Al–2Mg–11TiO2 composites", Wear 258, 2005, 759–767.

[5.] D. Mandal, B.K. Dutta, S.C. Panigrahi, "Wear properties of copper-coated short steel fiber reinforced stir cast Al–2Mg alloy composites", Wear 265, 2008, 930–939.

[6.] M. BakiKaramıs, Fehmi Nair, "Effects of reinforcement particle size in MMCs on extrusion die wear", Wear 265, 2008, 1741–1750.

[7.] T.V.S. Reddy, D.K. Dwivedi, N.K. Jain, "Adhesive wear of stir cast hypereutectic Al–Si–Mg alloy under reciprocating sliding conditions", Wear 266, 2009, 1–5.

[8.] Luca Casamichele, FabrizioQuadrini , Vincenzo Tagliaferri, "Non-destructive evaluation of local mechanical properties

of Al die cast large components by means of FIMEC indentation test" , Measurement 40, 2007, 892–897.

[9.] M. Emamy, M. Mahta, J. Rasizadeh, "Formation of TiB2 particles during dissolution of TiAl3 in Al–TiB2 metal matrix composite using an in situ technique", Composites Science and Technology 66, 2006, 1063–1066.

[10.] X.J. Wang, K. Wu, W.X. Huang, H.F. Zhang, M.Y. Zheng, D.L. Peng, "Study on fracture behavior of particulate reinforced magnesium matrix composite using in situ SEM", Composites Science and Technology 67, 2007, 2253–2260.

[11.] T.P.D. Rajan, R.M. Pillai, B.C. Pai, K.G. Satyanarayana, P.K. Rohatgi, "Fabrication and characterisation of Al–7Si–0.35Mg/fly ash metal matrix composites processed by different stir casting routes", Composites Science and Technology 67,2007, 3369–3377.

[12.] L. Ceschini, G. Minak, A. Morri, "Forging of the AA2618/20 vol.% Al2O3p composite: Effects on microstructure and tensile properties", Composites Science and Technology 69, 2009, 1783–1789.

[13.] S. Naher, D. Brabazon, L. Looney, "Simulation of the stir casting process", Journal of Materials Processing Technology 143–144, 2003, 567–571.

[14.] S.M. Olhero, J.M.F. Ferreira, "Rheological characterisation of water-based AlN slurries for the tape casting process", Journal of Materials Processing Technology 169, 2005, 206–213.

[15.] S. BalasivanandhaPrabu, L. Karunamoorthy, S. Kathiresan, B. Mohan, "Influence of stirring speed and stirring time on distribution of particles in cast metal matrix composite", Journal of Materials Processing Technology 171,2006, 268–273.

[16.] YucelBirol, "A357 thixoforming feedstock produced by cooling slope casting", Journal of Materials Processing Technology 186, 2007, 94–101.

[17.] K. Mahadevan, K. Raghukandan, B.C. Pai, U.T.S. Pillai, " Influence of precipitation hardening parameters on the fatigue strength of AA 6061-SiCp composite", journal of materials processing technology 198, 2008, 241–247.

[18.] Mohamed A. Taha, Nahed A. El-Mahallawy, Ahmed M. El-Sabbagh, "Some experimental data on workability of aluminiumparticulate-reinforced metal matrix composites",journal of materials processing technology 202, 2008,380–385.

[19.] *T*. Sornakumar, A. Senthil Kumar, "Machinability of bronze–alumina composite with tungsten carbide cutting tool insert, journal of materials processing technology 202, 2008, 402–405.

[20.] Arda Cetin, Ali Kalkanli, "Effect of solidification rate on spatial distribution of SiC particles in A356 alloy composites", journal of materials processing technology 205, 2008, 1–8.